The Cryosphere, 7, 889–904, 2013
www.the-cryosphere.net/7/889/2013/
doi:10.5194/tc-7-889-2013

The Cryosphere Open Access

Quantifying present and future glacier melt-water contribution to runoff in a central Himalayan river basin

M. Prasch[1], **W. Mauser**[1], **and M. Weber**[2]

[1]Department of Geography, LMU Munich, Germany
[2]Commission for Geodesy and Glaciology, Bavarian Academy of Sciences and Humanities, Munich, Germany

Correspondence to: M. Prasch (m.prasch@lmu.de)

Received: 23 September 2012 – Published in The Cryosphere Discuss.: 29 October 2012
Revised: 22 March 2013 – Accepted: 3 May 2013 – Published: 28 May 2013

Abstract. Water supply of most lowland cultures heavily depends on rain and melt water from the upstream mountains. Especially melt-water release of alpine mountain ranges is usually attributed a pivotal role for the water supply of large downstream regions. Water scarcity is assumed as consequence of glacier shrinkage and possible disappearance due to global climate change (GCC), in particular for large parts of Central and Southeast Asia. In this paper, the application and validation of a coupled modeling approach with regional climate model (RCM) outputs and a process-oriented glacier and hydrological model is presented for the central Himalayan Lhasa River basin despite scarce data availability. Current and possible future contributions of ice melt to runoff along the river network are spatially explicitly shown. Its role among the other water balance components is presented. Although glaciers have retreated and will continue to retreat according to the chosen climate scenarios, water availability is and will be primarily determined by monsoon precipitation and snowmelt. Ice melt from glaciers is and will be a minor runoff component in summer monsoon-dominated Himalayan river basins.

1 Introduction

Water supply of most lowland cultures heavily depends on rain and melt water from the upstream mountains, because mountain watersheds can store considerable amounts of precipitation as snowpack and glaciers (Viviroli et al., 2007). Its delayed release through snowmelt and glacier-ice melt can augment river runoff during dry periods (Jansson et al., 2003, Viviroli et al., 2007, Weber et al., 2010) with ice melt often being the last water source after the melt-out of snow. Especially melt-water release of glaciers in the Alps, the Himalaya and other alpine mountain ranges, is usually attributed a pivotal role for the water supply of large downstream regions (Baraer et al., 2012; Barnett et al., 2005; Bookhagen and Burbank, 2010; Collins and Tayler, 1990; Cruz et al., 2007; Huss et al., 2008; Huss, 2011; Moore et al., 2009; Pellicciotti et al., 2012). But snowpack and glaciers are among the land surface compartments most susceptible to global climate change (GCC). Glacier retreat has attracted wide public interest and serves as symbol for the impact of GCC. As consequence of glacier shrinkage and possible disappearance water scarcity is assumed (Cruz et al., 2007) due to GCC, in particular for large parts of Central and Southeast Asia (Barnett et al., 2005; Casassa et al., 2009; Cruz et al., 2007; Singh et al., 2006; Xu et al., 2009). Especially in High Asia this was brought into focus by the IPCC (Intergovernmental Panel on Climate Change) statement on Himalayan glacier retreat and its assumed consequences for water availability (Cruz et al., 2007). Despite recent studies pointing to the differing influences of ice-melt water on runoff due to regionally varying climatic and hydrological conditions along the Hindu Kush–Himalayas (Bolch et al., 2012; Immerzeel et al., 2010, 2012; Kaser et al., 2010; Kääb et al., 2012; Pellicciotti et al., 2012; Rees and Collins, 2006; Thayyen and Gergan, 2010), the future rate of recession of Himalayan glaciers as well as their present and future role for the downstream regions remain controversial.

The studies address the influence of ice melt in Asia on runoff either only qualitatively (Barnett et al., 2005), for hypothetical catchments (Rees and Collins, 2006), at almost continental scales (Bookhagen and Burbank, 2010;

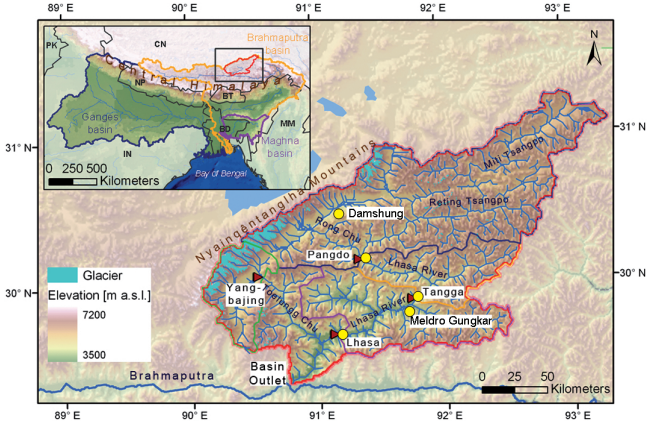

Fig. 1. Location of the Lhasa River basin in the central Himalaya and basin characteristics. The runoff gauges and the sub-basins analyzed in detail are marked with red triangles, the meteorological stations are marked with yellow circles and both are labeled (see also Supplement Table S1).

Immerzeel et al., 2010) or at small scales (Immerzeel et al., 2012). Some results are limited to present climatic conditions (Bookhagen and Burbank, 2010; Kaser et al., 2010; Pellicciotti et al., 2012; Thayyen and Gergan, 2010). This is also the case for the important analysis of changes in runoff in relation to glacier volume and area changes (e.g., Collins and Taylor, 1990; Huss et al., 2008; Jansson et al., 2003; and Moore et al., 2009) or future impacts are estimated in using a hypothetical development of climate and glaciers (e.g., Baraer et al., 2012) and no future climate model outputs. Different approaches, e.g., using the glacier mass balance to calculate glacier melt water release (e.g., Huss et al., 2008), often do not have a high temporal resolution and do not consider melt water release in the case of a balanced mass balance. Although the negative mass balance in the ablation area is balanced by the positive mass balance in the accumulation area, melt water is released in the lower parts. Detailed studies of the ice-melt contribution to runoff in relation to snowmelt and the other water balance components and of their changing composition due to GCC are needed to assess the current and future role of glaciers for downstream water management (e.g., Collins and Taylor, 1990; Huss et al., 2008; Kaltenborn et al., 2010; Jansson et al., 2003; Moore et al., 2009; Viviroli et al., 2011). They are, so far, rare in monitored regions like the Alps (Weber et al., 2010) and not available in remote regions as the Himalayas. Since there is no feasible method to distinguish river water according to its generation at the scale of large watersheds and because GCC deals with the future, model studies, properly validated with recorded data, are currently the only feasible approach to quantify the contributions of rainfall, snow- and ice melt to river runoff.

We present a model-based analysis of the temporal dynamics and spatial pattern of the rainfall, snow- and ice-melt contribution to river runoff under past and future climatic conditions for the Lhasa River basin (LRB) in the central Himalaya (Fig. 1, Sect. 2). To account for the specific and unique role of the glaciers for the downstream regions, we wanted to quantify the contribution of glacier ice-melt water to river runoff not only for the highly glacierized head watersheds but also for the downstream regions where people usually live and use the water. The results presented here are based on the approach developed in the integrative research projects GLOWA-Danube (GLObal change of the WAter cycle; www.glowa-danube.de) and BRAHMATWINN (Flügel, 2011) to study the impacts of climate change on water availability. The full model chain with PROMET (Processes of Radiation, Mass and Energy Transfer), SCALMET and SURGES (SUbscale Regional Glacier Extension Simulation) was already applied in the Upper Danube River basin with excellent data availability and validated in detail (Marke et al., 2011a, b; Mauser and Bach, 2009; Weber et al., 2010). General hydrological results were presented in Prasch et al. (2011a) for the Upper Brahmaputra River basin. Here, the application and validation of the coupled modeling approach with regional climate model (RCM) outputs and a process-oriented glacier and hydrological model is explained for the central Himalayan LRB despite scarce data availability (Sects. 3, 4). Then, the results are shown in depth: the spatial contribution of ice melt to river runoff along the river network of the LRB (Sect. 5.1), the amount of ice-melt water related to other water balance components (Sect. 5.2) and the timing of the melt contribution in its seasonal course (Sect. 5.3) for past and future climatic conditions from 1971–2080.

2 Study area

The LRB was chosen as a basin, being representative for a glacierized, complex head watershed of the Brahmaputra in High Asia with varying physio-geographic conditions. The Brahmaputra is together with the Ganges a major water source for approximately 300 million people in the lowlands in India and Bangladesh. The Lhasa River is the largest tributary in the middle reach of the mountainous Upper Brahmaputra with a drainage area of 32 800 km^2 (Fig. 1). The location on the Tibetan Plateau characterizes the physio-geographic conditions of the basin. The relief ranges from 3 535 m a.s.l. at the conjunction with the Brahmaputra up to 7 162 m a.s.l. at the peak of the Nyainqêntanglha Mountains, forming the northwestern watershed. Most glaciers in the LRB are found along this mountain range, one of the main glacierized areas of Central Asia (Yao et al., 2006), due to their altitude and orientation to the southeast from where the monsoon triggers orographic precipitation. Altogether 670 km^2, equating to 2 % of the total basin area, were glacierized in 1970 according to the Chinese Glacier Inventory (World Data Center For Glaciology and Geocryology, 2009). During the last decades a continuous retreat

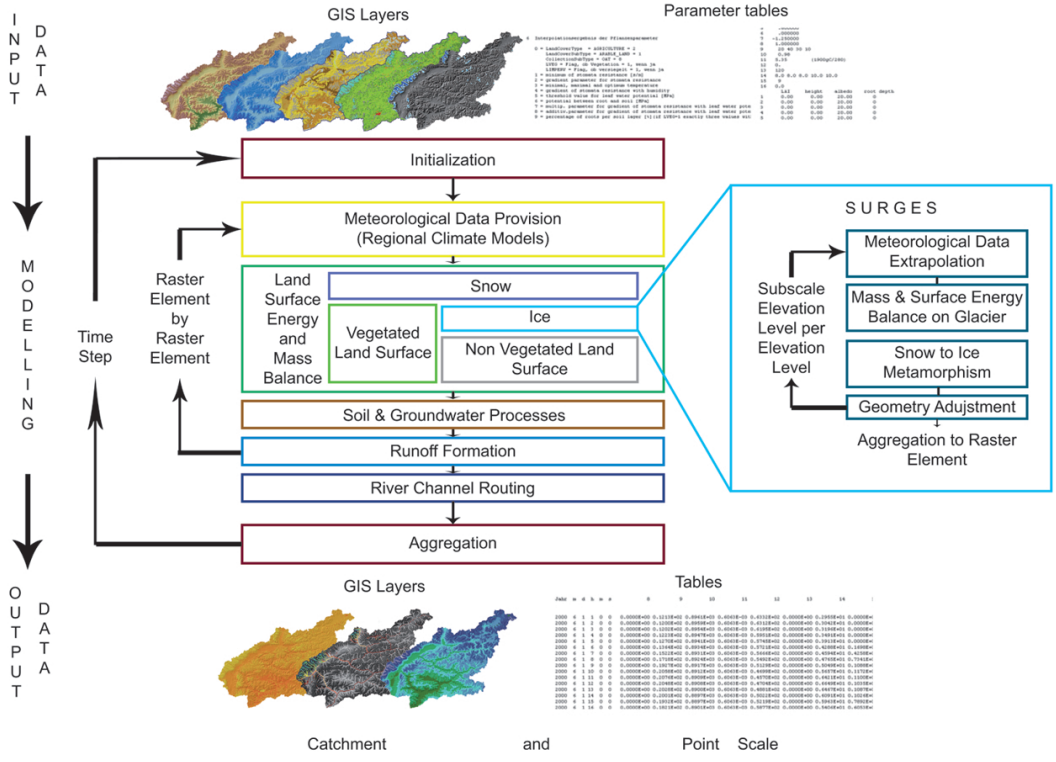

Fig. 2. Modeling approach. Scheme of implementation of the glacier model SURGES into PROMET, describing the spatial and temporal modeling cycle through the model components.

was recorded, similar to most parts of the Tibetan Plateau (Bolch et al., 2010; Li et al., 2011; Yao et al., 2007; Zhou et al., 2010). From 1970 to 2000, about 6 to 10 m w.e. (water equivalent) (Frauenfelder and Kääb, 2009; Kääb et al., 2008) melted away on average.

Climatic conditions in the LRB are determined by a strong seasonal course of the precipitation, which falls during the monsoon months in summer (430–520 mm a^{-1} (see also Table 2), 90 % falling from June to September). Mean annual air temperatures vary between –9 °C in the Nyainqêntanglha Mountains and +10 °C in the Lhasa River valley near the river's mouth. Due to the pronounced wet season during the summer monsoon and the dry season lasting the rest of the year, the runoff shows a clear seasonal cycle, with the flood peak reached in August. About 90 % of the mean annual runoff is observed between May and November, whereas in the winter season, runoff is low.

The coincidence of the ablation period and the monsoon season in summer largely determines the importance of glacier melt for water availability in the LRB similar to large, summer-monsoon dominated areas in the Himalayas, because melt water is of higher importance during dry periods and vice versa. In contrast to man-made reservoirs, snow and ice reservoirs are filled or emptied by natural processes in either a cyclic or anti-cyclic behavior, and therefore cannot be managed for downstream agriculture, hydropower, industry and households. If snow- and ice melt occur during the rainy season (cyclic behavior), they may add a small fraction to the large amount of runoff generated by heavy rainfall. When snow- and ice reservoirs melt during the dry season (anti-cyclic behavior), the generated runoff can be used to compensate potential water shortages.

The basin is only 2 % glacierized as of 1970. Nevertheless it was chosen, because the study wants not only to analyze the contribution of glacier melt water in the highly glacierized head watersheds. It also wants to analyze the influence of ice melt in the downstream regions, where usually people live and use water. Despite scarce data availability (Supplement Table S1 shows details of the observed meteorological and discharge data at the stations illustrated in Fig. 1) the successful application of a coupled modeling approach with RCM outputs and a process-oriented glacier and hydrological model can be demonstrated.

3 Methods

3.1 Model description

In our modeling approach (see Fig. 2) the PROMET watershed model (Mauser and Bach, 2009) is coupled with the SURGES glacier model (Weber et al., 2010) to clarify the influence of glacier melt water on river runoff in a Himalayan

river basin. In order to quantify the contribution of glacier melt water to river runoff not only for the highly glacierized head watersheds, but also for the downstream regions where people usually live and use the water, the full water balance components of a heterogeneous, large-scale river basin have to be taken into account. Therefore the models consider the water flows in vegetation, soils and river channels and the complete rainfall–runoff, snow and ice dynamics (Eq. 1):

$$Q = \mathrm{R} + \mathrm{S} - \mathrm{E} + \Delta\mathrm{GS} + \Delta\mathrm{SS} + \Delta\mathrm{IS}, \quad (1)$$

where Q is runoff, R is rainfall, S is snowfall, E is evapotranspiration, ΔGS is changes in groundwater storage, ΔSS is changes in snow storage, and ΔIS is changes in ice storage. Particularly evapotranspiration and the complex interactions of rainfall and snowmelt forming surface runoff, infiltrating into the soil and groundwater, forming interflow and base flow are important for runoff generation in the large downstream areas. Together with the melt-water release of the glacier ice the determination of the importance of ice-melt water throughout a mesoscale river basin is enabled. This is the underlying motivation to couple a complex hydrological model with a glacier mass- and energy-balance model. The small-scale processes leading to melt-water release on the heterogeneous surfaces of mountains and glaciers are considered by SURGES using a subscale approach in calculating the surface mass and energy balance of all glaciers in the basin. Accordingly these processes are calculated on a scale, which is finer than the applied process scale of the PROMET watershed model and parameterizes the subscale terrain using an area–elevation ice thickness classification table (see Sect. 3.1.3).

Furthermore, the method should allow determining the relevance of ice melt among the other water balance components. Consequently, we separated ice- and snowmelt in the entire basin. The term "snowmelt" is seen in a purely physical sense as "snow that melts at the surface of a snow cover" be it on the glacier or not. Therefore it consists of both, snowmelt from non-glacierized and glacierized parts of the basin. On each location on a glacier, ice melt can only set in after all snow has melted and the ice is exposed to energy transfer from radiation and/or the atmosphere.

A consistent meteorological data set (near-surface air temperature, precipitation, air humidity, wind speed, incoming shortwave and longwave radiation in a temporal resolution of 1 h) is required for each raster element to run the models. Therefore, the scaling tool SCALMET (Marke et al., 2011a, b) is applied to downscale outputs of RCMs during runtime.

3.1.1 The PROMET watershed model

The PROMET model used in this study was developed in order to study the impacts of climate change on the water balance in heterogeneous, large-scale river basins ($A \sim 100\,000\,\mathrm{km}^2$). PROMET runs with a temporal resolution of 1 h and is a spatially distributed model. It is based on physical principles and the mass and energy balances are closed. The model is not calibrated to measured runoff and the parameterizations are invariant in space and time across the whole basin. Varying climatic conditions and hydrological regimes of complex catchments (e.g., mountain head watersheds and large river valleys in the forelands) are modeled synchronously by PROMET (Mauser and Bach, 2009). The model was successfully applied in the complex river basin of the Upper Danube in central Europe ($A = 77\,000\,\mathrm{km}^2$) with comparably good data availability under past and future climate conditions. Due to its characteristics PROMET fulfills the requirements for impact studies of climate change on the regional scale (Mauser and Bach, 2009). The local heterogeneities in the LRB are considered through a model raster with a resolution of 1×1 km.

3.1.2 The scaling tool SCALMET

In this study the scaling tool SCALMET (Marke et al., 2011a, b) applies statistical downscaling functions without any further bias correction to expand from the RCM scale (45×45 km) to the scale of the hydrological simulations (1×1 km). Topographical information (elevation, slope, aspect) is included in order to consider subgrid-scale heterogeneities and related natural climate gradients, which are particularly important in mountainous terrain. For each time step, the elevation dependency of meteorological variables, strongly varying with terrain elevation, e.g., air temperature or air humidity is analyzed. A regression function is determined, which is then applied to adjust these variables. The scaling methods applied consist of bilinear interpolation and statistical downscaling with conservation of mass and energy (Marke et al., 2011b). For physical downscaling, submodels are implemented to downscale wind speed, shortwave and longwave radiation (Liston and Elder, 2006; Izimon et al., 2003) to account for subscale heterogeneities within the remapping process (Marke, 2008). Since the temporal resolution of the regional climate model used in this study is 3 h, a temporal interpolation routine is also implemented. In these cases a cubic spline function is applied to all meteorological parameters except precipitation. The latter is classified under short events for a single recording and under long-term events for consecutive observations. Afterwards, the precipitation is distributed to the hours before the single event using a Gaussian distribution, or equally distributed in time for the continuous case following Mauser and Bach (2009). This routine runs prior to the downscaling processes. In this study the meteorological data precipitation, air temperature, air humidity, incoming shortwave and longwave radiation, air pressure and wind speed of the RCM are downscaled by SCALMET. The downscaling techniques implemented in SCALMET are based on physical and statistical approaches, so they are completely general and can be applied without any further parameterization in various regions. For further details refer to Marke et al. (2011a, b).

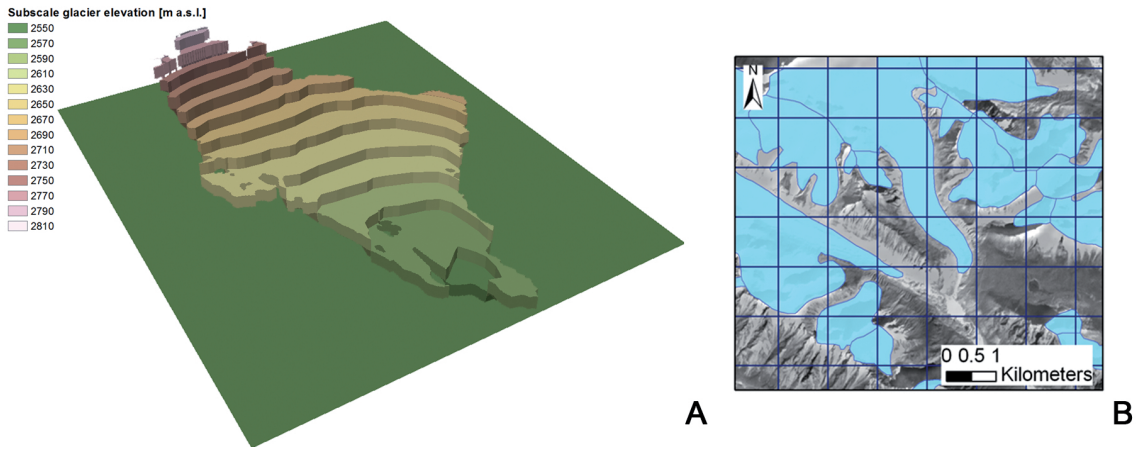

Fig. 3. Approximation of area-elevation distribution of a glacier by SURGES for one raster element **(A)** and elevation levels of a glacier covering several raster elements **(B)**.

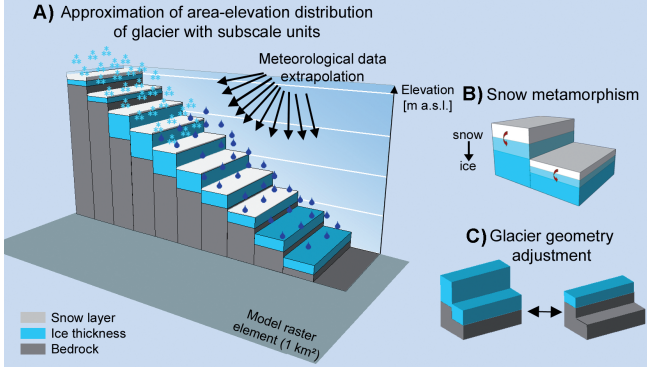

Fig. 4. Scheme of subscale approach of the glacier model SURGES (modified after Prasch et al., 2011a, p. 63).

3.1.3 The SURGES glacier model

Concerning the strong variation with elevation of the processes, SURGES uses an area–elevation distribution with subscale units (for the LRB elevation levels with intervals of 100 m are applied) (Fig. 3a) to approximate the complex terrain of mountain glaciers within all glacierized 1 km^2 raster elements of the full river basin. If a glacier covers several raster elements (Fig. 3b) the elevation belts of one glacier are spread over several raster elements. Each subscale unit is characterized by a homogenous ice thickness and surface elevation. The subscale approach thus enables the coexistence of accumulation zones at the higher altitudes and ablation zones at the lower altitudes within one raster element (Fig. 4a). The algorithms of SURGES to calculate accumulation and melt rates are designed to use data as measured at a local climate station as input. Hence, the meteorological data for precipitation, air temperature, air humidity, incoming shortwave and longwave radiation, air pressure and wind speed, provided by SCALMET, has to be extrapolated to the elevation levels. Therefore air temperature, air pressure, wet bulb temperature (for differentiation of rain from snowfall by iteratively solving the psychrometer formula) and the wind speed on the glacier for air temperatures above 0 °C (a katabatic flow over glaciers, which is caused by the differences in the density of air between the snow-free surrounding areas of a glacier and the comparatively cold glacier surface, which is very common over melting surfaces) are extrapolated due to the different elevations at the subscale glacier belts. All the other meteorological variables, e.g., precipitation or incoming radiation, are assumed to be constant throughout the raster element and are taken from SCALMET without any adaptation. Details of the meteorological data provision are presented in the Supplement.

Due to a threshold wet-bulb temperature a distinction is made between rain and snowfall. The latter accumulates until melt sets in. In order to determine the ablation, mass and surface energy balance, taking into account the radiation balance, the latent and sensible heat fluxes, and the energy supplied by solid or liquid precipitation of snow and ice are calculated for every subscale unit to calculate the amount of glacier melt, which largely occurs on snow-free glacier areas (Prasch et al., 2008; details also in the Supplement). The mass change conducted by sublimation/resublimation is also calculated by SURGES. As long as snow covers the glacier surface it is protected against melt. The melt water (first from snow and after snow vanishes from glacier ice) is aggregated for each raster element and injected into river runoff within the routing component of PROMET. Snow (Fig. 4b, white, above) to ice metamorphism is considered in partly adding snow, which outlasted a defined number of ablation periods, (Fig. 4b, blue in between) to the ice layer (Fig. 4b, light blue, below). In the test site of the Lhasa River catchment, not only accumulation but also ablation takes place during the monsoon. Furthermore, alternating melting and refreezing was observed up to 5 800 m a.s.l. (Kang et al., 2007).

These processes accelerate snow metamorphism. Thus, after a period of one year, similar to the estimation of Kang et al. (2007), half of the snow layer is transformed to ice in this study. Even though firn is not distinguished specifically, changes with respect to the energy balance are taken into account by the simulation of changes in the albedo, varying between 0.5 (snow-free ice) and 0.9 (freshly fallen snow) (further details in the Supplements).

Finally, glacier geometry is adjusted both in the case of melt out or growth of the ice reservoir on different elevation levels in reducing or respectively increasing glacier area (Fig. 4c). In the first case, the ice on an elevation level melts away and then the glacier area is reduced by the area of the elevation level (Fig. 4c, left to right). In the second case, snow accumulates and ice is build on an ice-free elevation level and then the glacier area is increased by the area of the elevation level (Fig. 4c, right to left). Since snow that accumulates at the higher elevation levels is transformed to ice as explained above and sublimation, evaporation and melt are taken into account, it does not accumulate endlessly, although the loss of ice thickness there is underestimated because of the missing consideration of subsidence caused by ice flow. Released melt water is aggregated for each raster cell and then redirected to the stream flow from all cells by PROMET's routing component as described in Mauser and Bach (2009). Additionally, the model chain is applied under future climate conditions, which are characterized in this region according to the climate model outputs by increasing temperatures and only slight changes in the amount of precipitation, so that glacier retreat goes along with a reduction of the ice flow. Although an ice flow model is not explicitly implemented, the approximation of glacier geometry changes is considered in a first step. Moreover, the complexity of the relevant processes requires detailed information about the glacier's geometry and cannot be simulated in a simple approach on the catchment scale. This is the reason why glacier changes are crudely considered in long-term studies (e.g., Rees and Collins, 2006).

3.1.4 Discussion of the modeling approach

Focusing on the effect of the processes in determining the melt-water release under changing climatic conditions throughout a complex mesoscale river basin in the presented modeling approach results in the neglect of some small-scale processes on the glacier so far. Wind-induced snow transport and the small-scale shading caused by the surrounding mountains, which principally facilitate the formation of glaciers in some cases, has so far been neglected. The effect of transporting ice from the accumulation to the ablation area due to the ice flow has so far been excluded, but the snow-to-ice metamorphism and glacier geometry changes are considered in a first step as well as sublimation. Accordingly, snow that accumulates at the higher elevation levels is transformed to ice and does not accumulate endlessly as explained in Sect. 3.1.3. Since the model chain is applied under future climate conditions which are characterized in this region according to the climate model outputs by increasing temperatures and only slight changes in the amount of precipitation, glacier mass balances are negative and consequently cause glacier geometry changes, which are considered. This process is partly compensated by the ice flow of large glaciers, which is so far not explicitly implemented. The enhancement of the model with an ice flow model is intended for future work.

The approach nevertheless enables the distributed simulation of the main processes for determination of the melt water release of all glaciers in a mesoscale river basin. The properties of each single glacier are considered in as much detail as possible by the approximation of the ice thickness area–elevation distribution. This includes capturing the small-scale glacier properties below the process scale of PROMET of 1×1 km for the simulation of energy and mass balances. Furthermore, the coexistence of rain- and snowfall, of the accumulation and ablation zones of a glacier and the neighboring non-glacierized areas on one raster element can be handled. Geometry changes in the glacier are considered in reducing the glacier area after the ice melt at given elevation levels, although the implementation of ice flow effects could improve the determination. Moreover, SURGES can be applied under past as well as future climatic conditions, since it is process oriented and uses universal constants and universal algorithms, which are invariant in space and time throughout the basin. Through the implementation of SURGES in PROMET, the influence of the melt water release of glaciers for the water balance can be determined in a spatially distributed way over the complete large-scale catchment, considering the full water balance processes. Finally, in applying the SCALMET tool, RCMs can be applied as meteorological input data. They make the application of the modeling approach independent of meteorological station data. This is especially important in remote mountain regions as is the LRB.

3.2 Input data

Outputs of the regional climate model COSMO-CLM (Climate Limited-area Modeling Community, 2012) for past and future are used as meteorological drivers. CLM, driven by the coupled ocean–atmosphere global climate model (GCM) ECHAM 5/MPI-OM (European Centre/Hamburg Model), was chosen, because it realistically simulates the 20th century South Asian monsoon compared to other GCMs following Kripalani et al. (2007). Additionally, ERA 40 (ECMWF 40 yr re-analysis) was applied for the past (particularly for the model validation) to reduce GCM simulation biases, since they are based on meteorological observations. The CLM outputs for air temperature and precipitation are bias corrected for the whole Upper Brahmaputra Basin (Dobler and Ahrens, 2008, 2010), using available station data. Then

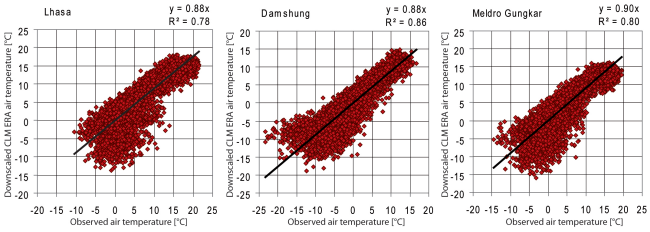

Fig. 5. Comparison of modeled (CLM ERA 40 driven SCALMET outputs) and observed daily air temperatures for the Lhasa, Damshung and Meldro Gungkar stations.

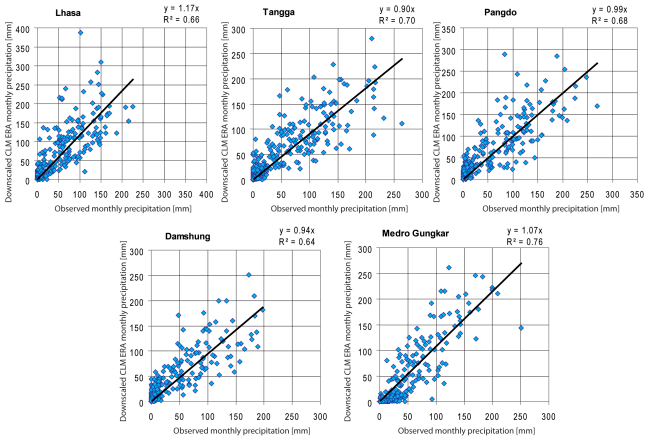

Fig. 6. Comparison of modeled (CLM ERA 40 driven-SCALMET outputs) and observed monthly precipitation for the Lhasa and Tangga (1971–2000), Pangdo (1976–2000) and Damshung and Meldro Gungkar stations (1980–2000).

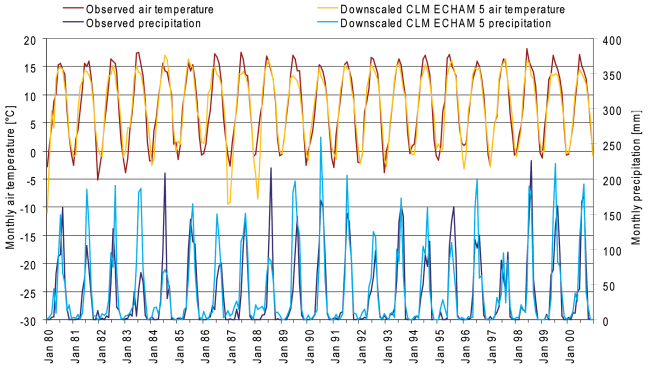

Fig. 7. Development of observed and modeled (CLM ECHAM 5 driven SCALMET outputs) monthly air temperature and precipitation at the Lhasa station for 1980–2000.

the CLM data were downscaled to the spatial resolution of 1×1 km through the scaling tool SCALMET (Marke et al., 2011a, b) without adding further bias correction. For all further model parameters we used open access data like SRTM (Shuttle Radar Topography Mission; Jarvis et al., 2006) and Aster (ERSDAC, 2009) digital elevation models, the NASA Terra/Modis land cover product (Boston University, 2004), the Harmonized World Soil Database (FAO et al., 2009) and the Chinese Glacier Inventory (World Data Center For Glaciology and Geocryology, 2009), which provides mean ice thickness for the glaciers in the LRB. The mean ice thickness is then modified considering surface slope (Haeberli and Hoelzle, 1995) and the thinning out of the glacier to its edges and front. Additionally, a digital terrain analysis was carried out with TOPAZ (Topographic Parameterization; Gabrecht and Martz, 1999) and field data were applied. Further details to the applied input data in the models can be found in Table 1 and in Prasch et al. (2011b).

4 Validation of the modeling approach in the Lhasa River basin

The models PROMET, SURGES and SCALMET have been developed and successfully applied within the integrative research project GLOWA-Danube (www.glowa-danube.de). Additionally, PROMET and SCALMET were applied in the Upper Brahmaputra Basin (Prasch et al., 2011a, b) to study the impacts of climate change on water availability within the framework of the project BRAHMATWINN (Flügel, 2011). The full model chain was already applied in the Upper Danube River basin and validated in detail (Weber et al., 2010; further details in the Supplement). Therefore, here the validation of the modeling approach in the LRB is shown. This includes validating with SCALMET downscaled air temperature and precipitation, glacier development, and runoff in the LRB.

4.1 Validation of air temperature and precipitation in the LRB

To validate the downscaled air temperature and precipitation sums in the LRB, the data recorded air temperature and precipitation data at five meteorological stations (Fig. 1, Table S1) are compared with the downscaled values after SCALMET is run. Both, CLM ERA 40 and CLM ECHAM 5 data are used as input for SCALMET in the validation, because ECHAM 5 driven SCALMET outputs, as driven by a climate model, cannot reproduce the chronology of the meteorological conditions contrary to ERA 40 data, which are based on observations. The SCALMET outputs of CLM ECHAM 5 should, however, reproduce the meteorological conditions and the climate signal. Consequently, the average values, the general seasonal course without matching single years and the trend of the data should be comparable to observed data. ERA 40 driven outputs should additionally represent the seasonal course of single years.

As shown in Table 2, the recorded air temperature is reproduced for the stations by both CLM model driven SCALMET outputs, except that in Damshung for the ECHAM 5 driven model run, where the temperature is overestimated by

Table 1. Required input data layers to run the models PROMET, SCALMET and SURGES and data sources for the Lhasa River catchment.

Input data set	Data source	Model
Watershed	Digital terrain analysis of SRTM with TOPAZ Garbrecht and Martz (1999)	PROMET
Elevation (m a.s.l.)	SRTM Jarvis et al. (2006)	PROMET
Surface slope (%)	Digital terrain analysis of SRTM with TOPAZ	PROMET
Surface aspect	Digital terrain analysis of SRTM with TOPAZ	PROMET
Land use/land cover classes	NASA TERRA/MODIS land cover product Boston University (2004)	PROMET
Soil texture classes	Harmonized World Soil Database FAO et al. (2009)	PROMET
Accumulated upstream area (km^2)	Digital terrain analysis of SRTM with TOPAZ	PROMET
Channel slope (%)	Digital terrain analysis of SRTM with TOPAZ	PROMET
Flow direction	Digital terrain analysis of SRTM with TOPAZ	PROMET
Channel width (m)	Deduced, based on field data	PROMET
Manning's roughness parameter	Deduced, based on field data	PROMET
Groundwater storage time (h)	Deduced, based on the digital terrain analysis of SRTM with TOPAZ	PROMET
Meteorological values (near surface air temperature, precipitation, air humidity, wind speed, incoming short- and longwave radiation)	COSMO-CLM outputs Climate Limited-area Modeling Community (2010), driven by the GCM ECHAM 5 %/MPI-OM and ERA 40 and downscaled with SCALMET	SCALMET/ PROMET/ SURGES
Subscale glacier area (m^2)	Chinese Glacier Inventory, World Data Center For Glaciology and Geocryology (2009)	SURGES
Subscale glacier elevation (m a.s.l.)	Aster GDEM ERSDAC (2009)	SURGES
Subscale glacier slope (%)	Aster GDEM ERSDAC (2009)	SURGES
Subscale ice thickness (m)	Deduced, based on WDC (2009) and ERSDAC (2009)	SURGES

Table 2. Validation of simulated CLM ERA 40 and CLM ECHAM 5 and observed mean values of air temperature and precipitation in the LRB.

	Air temperature (°C)					Precipitation sum (mm)				
Station and time period	Observation	Downscaled CLM data (driven by ERA 40)	Δ	Downscaled CLM data (driven by ECHAM 5)	Δ	Observation	Downscaled CLM data (driven by ERA 40)	Δ	Downscaled CLM data (driven by ECHAM 5)	Δ
Lhasa (1980–2000)	8.1	7.2	−0.9	7.9	−0.2	426	584	158	524	97
Meldro Gungkar (1980–2000)	6.0	5.3	−0.7	6.0	0.0	548	532	−16	481	−67
Damshung (1980–2000)	1.8	1.7	−0.1	2.4	0.6	464	543	80	511	48
Pangdo (1976–2000)			no data			538	647	91	587	41
Tangga (1971–2000)			no data			517	561	44	513	−4

0.6 K. The mean precipitation sum of Damshung and Pangdo is overestimated by the CLM ECHAM 5 driven SCALMET outputs, but the deviations are within 10 %, whereas in Lhasa the overestimation reaches 22 %. The precipitation sum is slightly underestimated for Meldro Gungkar and Tangga. In comparison to the CLM ERA 40 driven SCALMET temperature and precipitation values, the deviations seen are smaller. The comparison of CLM ERA 40 driven SCALMET outputs with observed daily air temperatures (Fig. 5) and monthly precipitation sums (Fig. 6) show that the seasonal course can be reproduced despite deviations. The exemplarily comparison of observed and modeled monthly air temperature and

Table 3. Quality criteria for modeled monthly and daily runoff ($m^3 s^{-1}$) for CLM ERA 40-driven model runs.

Quality criteria	Monthly runoff			Daily runoff		
	Lhasa (1971–2000)	Pangdo (1976–2000)	Tangga (1971–2000)	Lhasa (1996–2000)	Pangdo (1996–2000)	Tangga (1997–2000)
Coefficient of determination R^{-2}	0.79	0.78	0.80	0.72	0.70	0.74
Slope of linear regression	1.37	1.30	1.29	1.00	0.92	0.93
Nash–Sutcliffe efficiency coefficient	0.31	0.39	0.48	0.67	0.70	0.73

Table 4. Validation of mean annual runoff ($m^3 s^{-1}$ for ERA 40- and ECHAM 5-driven model runs).

Period	Mean annual runoff ($m^3 s^{-1}$)	Lhasa *R*	Pangdo *R*	Tangga *R*
1971–2000	Observed	279	196	237
	ERA 40	408	270	321
	Δ ERA 40 (%)	+46	+37	+36
	ECHAM 5	351	233	278
	Δ ECHAM 5 (%)	+26	+19	+17

precipitation of the CLM ECHAM 5 driven SCALMET outputs are illustrated for the station Lhasa in Fig. 7. The seasonal cycles are captured by the model output, with the monsoon precipitation during the summer months and the dry winters, although there are overestimations of precipitation during the pre-monsoon time in April and May, taking into account that the annual values cannot be reproduced by a climate model. The comparison of the monthly simulated and observed values also shows modeling of a reasonable range of minimum and maximum values. Two January temperatures, however (1987, 1988), are simulated at a clearly lower level than all observations. Consequently, the mean meteorological conditions are reproduced by the CLM ECHAM 5 model run, particularly when considering the coarse resolution of the CLM outputs. Taking into account technical difficulties in precipitation observation and the resulting deviations, the average results seem to be reasonable.

4.2 Validation of glacier development in the LRB

As part of the Brahmatwinn project, a detailed glacier change study for the Lhasa River basin was conducted by comparing multi-temporal optical remote sensing data from the Landsat and ASTER sensors with the Chinese Glacier Inventory (Frauenfelder and Kääb, 2009; Kääb et al., 2008). A total change of −21 % in glacier area from 1970 to 2000 was found. Using various area–volume relations a mass balance change of −0.2 to −0.3 m w.e. per year was estimated (Frauenfelder and Kääb, 2009; Kääb et al., 2008).

For the past 30 yr, a decrease of 20 % (CLM ECHAM 5) of the glacier area is modeled. This is within the range of the observed glacier area reduction. For the ice-water reservoir, an average mass loss of 0.3 m (CLM ECHAM 5) is calculated. In comparison with the results for this area, the mass loss is consistent.

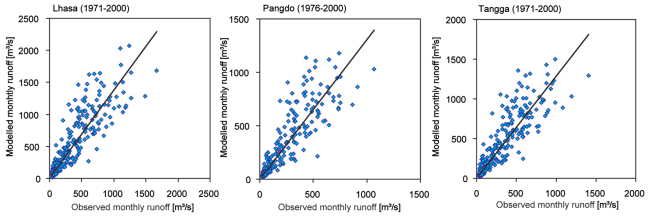

Fig. 8. Comparison of observed and modeled monthly runoff.

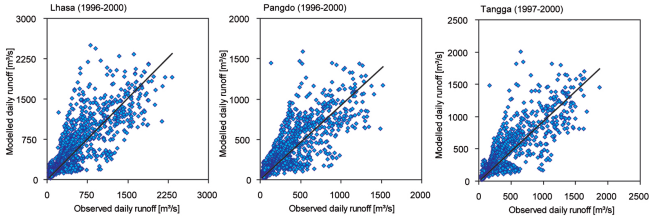

Fig. 9. Comparison of observed and modeled daily runoff (Lhasa data are from Prasch et al., 2011a, p. 66).

4.3 Validation of runoff in the LRB

To validate the simulated runoff in the Lhasa River basin, two model runs, driven by downscaled CLM ERA 40 and CLM ECHAM 5 meteorological data, were carried out from 1 January 1971 to 31 December 2000, on a temporal resolution of 1 h. Due to PROMET's spin up, the first model year is not considered in the validation. The model results are compared to runoff observations at three gauging stations in the LRB (Fig. 1). Figures 8, 9, 10 and 11 show the comparison of

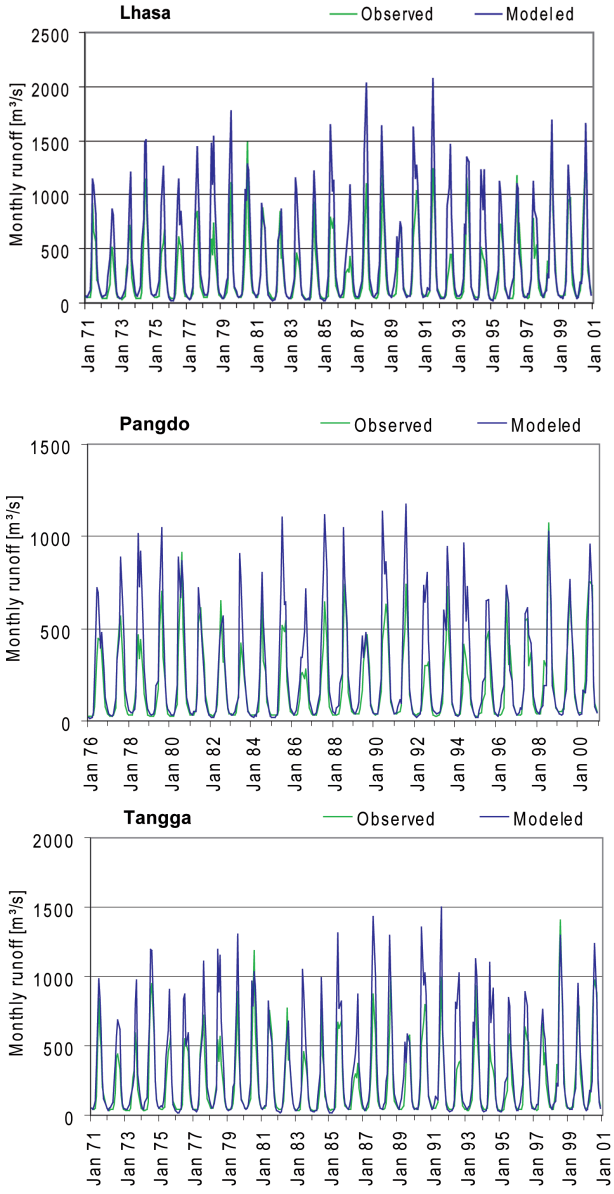

Fig. 10. Development of monthly observed and modeled runoff at Lhasa, Pangdo and Tangga gauges from 1971/1976–2000.

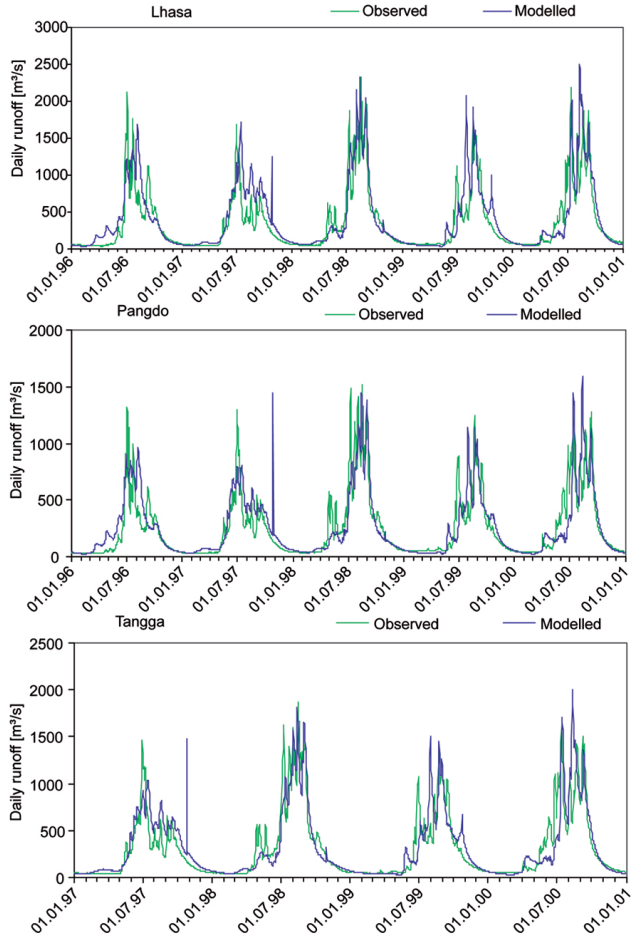

Fig. 11. Development of daily observed and modeled runoff (Lhasa data are from Prasch et al., 2011a, p. 66).

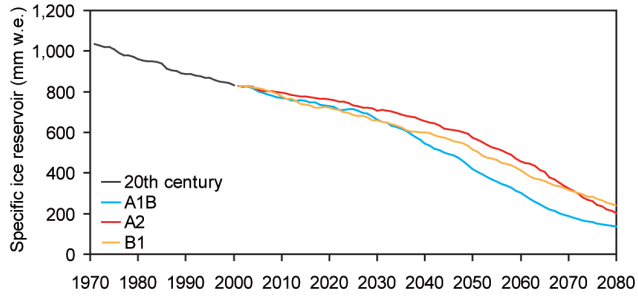

Fig. 12. Modeled development of the specific ice reservoir in the LRB from 1970 to 2080. The evolution is shown for the past (1970–2000) and for the IPCC SRES-A1B, -A2 and -B1 emission scenarios (2000–2080). Detailed values can be found in Supplement Table S3.

daily and monthly runoff values for the CLM ERA 40 driven model run together with quality criteria in Table 3, whereas for the CLM ECHAM 5 and ERA 40 driven results the mean annual runoff is validated as climate signal (Table 4). The validation of modeled runoff shows an overestimation during the summer months, but this overestimation changes during the validation period from 1971 to 2000. While it is large in the 1970s and 1980s, it is clearly reduced in the 1990s. The reason for the change can be found in the input of the amount of precipitation which is then also in better accordance with the observations as shown in the Supplement Table S2. Although there are biases, the seasonal runoff course is reproduced by the model, especially when taking into account the coarse spatial and temporal resolution of the CLM output data as meteorological drivers. Furthermore, the modeling approach is not calibrated to observed runoff in order to be applicable also for changing future watershed conditions or climates.

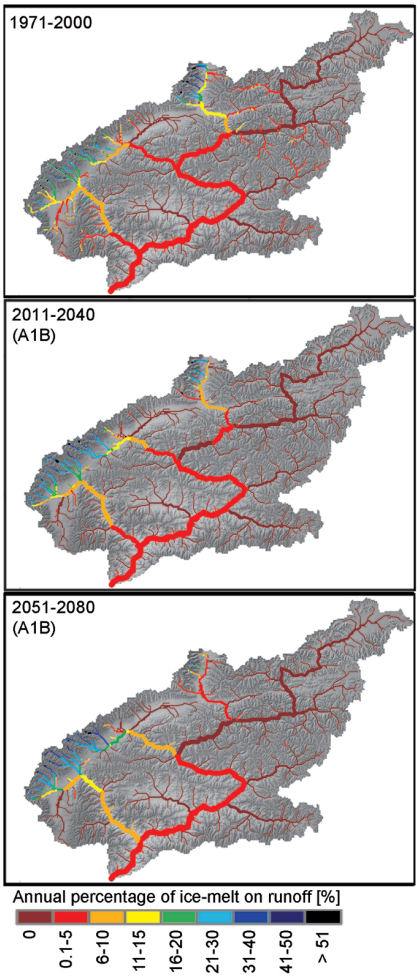

Fig. 13. Mean annual runoff fraction of ice melt throughout the river network. Colored rivers contain ice-melt water; no ice melt contributes to runoff of brown rivers. The percentage is shown for rivers with average runoff above 0.5 $m^3 s^{-1}$ for the past (1971 to 2000) and the future SRES-A1B scenario periods (2011–2040 and 2051–2080); river width symbolizes runoff quantity between 0.5 and 450 $m^3 s^{-1}$.

5 Results

The seasonal contribution of snow- and ice melt to total runoff is analyzed for the past 30 yr and the IPCC SRES-A1B, -A2 and -B1 emission scenarios (Nakićenović et al., 2000) until 2080. Figure 12 shows the development of the modeled total ice volume in the LRB between 1970 and 2080 for the three selected emission scenarios. The spatial distribution in the LRB for 2000 and 2080 is shown in Supplement Fig. S1, detailed numbers of future glacier change are presented in Supplement Table S3. The observed continuous glacier retreat during the last decades (Bolch et al., 2010, Frauenfelder and Kääb, 2009; Kääb et al., 2008; Yao et al., 2007) will continuously proceed regardless of the selected scenario, but glaciers will not completely disappear until 2080, because the large ice reservoirs between altitudes from 5600 to 6100 m a.s.l. and glaciers extending up to 7200 m a.s.l. resist melting for a long time. Since the results do not principally differ among the scenarios, we focus on the A1B analysis in the following.

5.1 Contribution of ice melt to river runoff along the river network

To determine the contribution of glacier ice-melt water, the model is run under two different model settings. In the first setting, glaciers are considered and ice melt is directly injected into the river channels. In the second setting, glacier volumes are set to zero. We consider, for each time step, the difference in runoff between the two model settings as the ice-melt runoff component. In order to specifically quantify the contribution of ice melt to total runoff, it is treated separately from snowmelt, which occurs contrary to ice melt throughout the whole basin. Divided by total runoff including ice melt, it represents the contribution of ice melt to total runoff, shown in Fig. 13. While ice melt amounts to more than 50 % of total runoff in the glacierized head watersheds, its contribution rapidly decreases as watershed area increases. In the larger tributaries ($A > 3000\,km^2$) and at the outlet of the LRB only 0.1–5 % of the water can be attributed to ice melt during the past period from 1971–2000.

In the future periods 2011–2040 and 2051–2080 the spatial patterns of the contribution of ice-melt water remain similar (Fig. 13). However, total melt out of glaciers occurs in the northeastern and southern areas of the LRB, which reduces ice-melt contribution to zero. Despite the continuous future reduction of glacierization (Figs. 12, S1), which would suggest a decreasing fraction of ice melt, it hardly changes in the main rivers and even slightly increases in the highly glacierized head watersheds, similar to trends analyzed for the Alps (Pellicciotti et al., 2010). In-depth analysis of this remarkable finding shows that the reason lies in an altitudinal shift of the snow conditions of about +500 to +1000 m because of rising air temperatures. This altitudinal shift extends the snow-free period by two to three months (Figs. 14, 15) and thereby increases ice melt per area and year. Since this shift is proceeding continuously, similar to glacier retreat, the simulated changes of the snow-free glacier area, decisive for ice melt, are small despite the shrinking overall areal extent of the glaciers. A detailed look at the modeled glaciers shows that the increasing ice melt compensates their shrinking areal extent and leads to an almost stable fraction of ice melt in the river runoff.

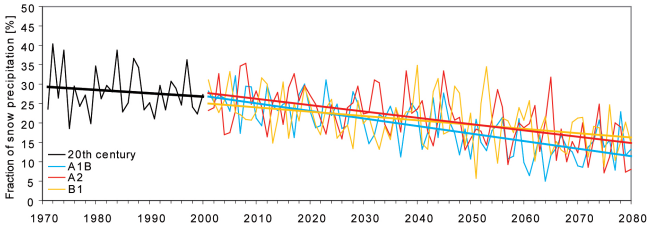

Fig. 14. Modeled development of the fraction of snow precipitation in the LRB.

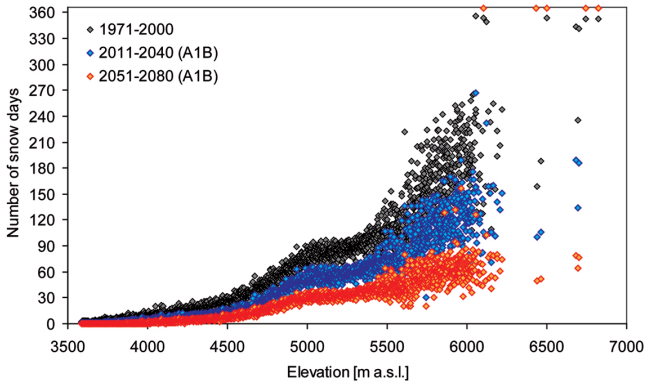

Fig. 15. Modeled number of snow days at different altitudes in the LRB.

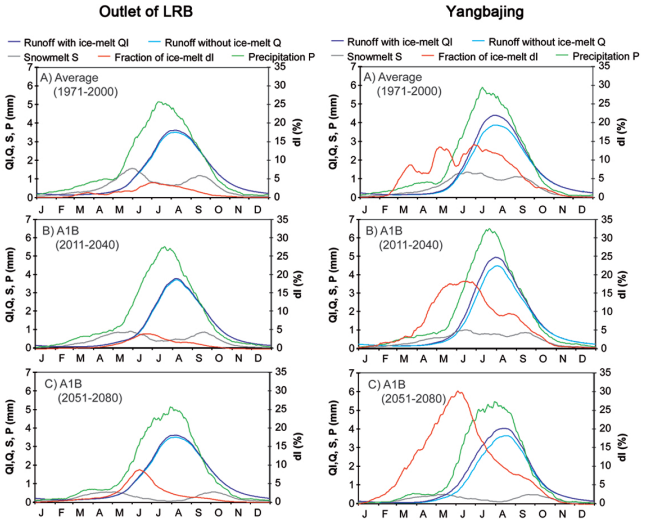

Fig. 16. Average annual dynamics of daily different runoff components at the outlet of the LRB (left) and at Yangbajing (right) (moving average over 30 days); river runoff with (blue) and without (cyan) ice melt (left y-axis) together with snowmelt water release of the basin (grey, left y-axis), precipitation (green, left y-axis) and fraction of ice melt (red, right y-axis) for the periods 1971–2000 **(A)**, 2011–2040 **(B)** and 2051–2080 **(C)** are shown (see also Supplement Fig. S2).

5.2 Ice melt related to other water balance components

The following analysis of all water balance components gives deeper insight. For each hourly model time step, runoff is composed of rainfall, snow- and ice melt, which, together with evapotranspiration and changes in snow, ice, soil and ground water storage close the water balance (see Eq. 1 and Supplement Tables S4, S5 and S6). Since long-term changes in soil water content and groundwater in the LRB are modeled to be below 1 %, they are neglected. To determine the relative contribution of ice melt in comparison to the other runoff and water balance components, we separated them for the five gauges in the LRB marked in Fig. 1. Table 5 shows that today about 30 % of the water in the LRB evaporates, which is in accordance with Sharma et al. (2000), whereas 70 % is released as runoff. The most important runoff component at the outlet today originates from snowmelt. Rainfall generates 40 % of the runoff whereas ice melt contributes between 2 and 3 % (max. 11 % at Yangbajing).

Under future climatic conditions, increasing evapotranspiration is modeled due to rising temperatures. Together with a slight decrease in precipitation this results in a considerable decrease in runoff at all gauges except at Yangbajing during both future periods. There, evapotranspiration increases only marginally and the modeled annual ice-melt contribution slightly increases because of the large decrease in snowmelt during both simulated future periods. The latter is due to the compensational effect described above. Consequently, the importance of ice melt will remain low at the outlet and in most parts of the LRB (see also Fig. 13).

5.3 The seasonal timing of melt contribution

A closer look at the seasonal dynamics of the runoff components in the LRB and at Yangbajing, which are shown in Fig. 16, creates additional insight into the possible future role of glaciers in the LRB for water supply of the downstream lowlands. The annual runoff course at the basin outlet in a daily resolution (Figs. 16, left; S2, left), averaged over the period from 1971–2000, shows a very distinct and consistent runoff maximum during the summer months caused by monsoon rainfall (Figs. 16a, S2D, left). Runoff is low during winter because of reduced precipitation, which predominantly falls and is stored as snow. The fraction of ice melt approaches zero during winter, since the glaciers are snow covered. Any melt during warm spells in winter occurs as snowmelt. With increasing temperatures in spring snowmelt sets in first, is infiltrated into the soil or evaporated into the atmosphere, and peaks in late May before monsoon precipitation fully sets in. At that time, the glacierized area is still protected from ice melt by a snow cover. As snow vanishes in high altitudes, ice melt starts to increase to a maximum of 5 % of total runoff until late June. Then, the increasing monsoon precipitation also increasingly causes snow to fall in high altitudes. This snow cover partly protects the glaciers from melting. Coincidently, increasing cloudiness reduces

Table 5. Fractions of past and future water balance components. Right circles show the water balance components evapotranspiration (yellow) and runoff (red); left circles show runoff components, rainfall (blue), snowmelt (white) and ice melt (cyan); the diameter of the circles reflects the magnitude of runoff (white – bluish, left) and evapotranspiration plus runoff which is similar to precipitation plus ice-storage changes (yellow – red, right) in the watersheds represented by the gauges in column 1 (see Fig. 1). The detailed water balance components can be found in the Supplement Tables S4, S5 and S6.

				1971–2000		2011–2040 (A1B)		2051–2080 (A1B)	
Gauge	Area (km^2)	Glacierization (1970) (%)	Water Quantity (mm)	Runoff Generation	Water Balance	Runoff Generation	Water Balance	Runoff Generation	Water Balance
Outlet	32 798	2.0	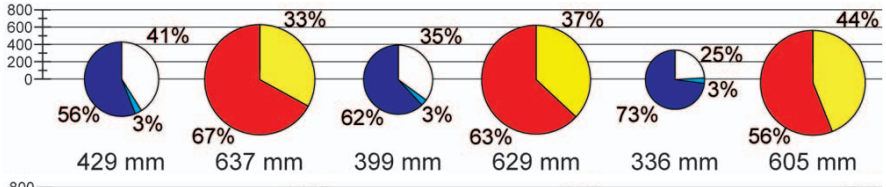						
Lhasa	26 339	1.3	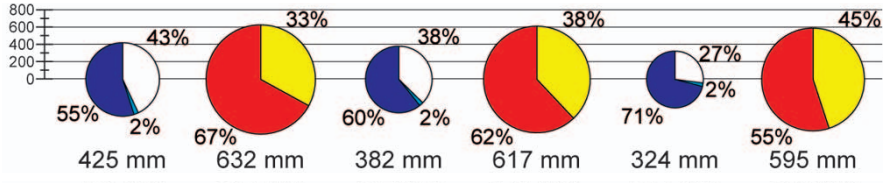						
Tangga	20 195	1.7	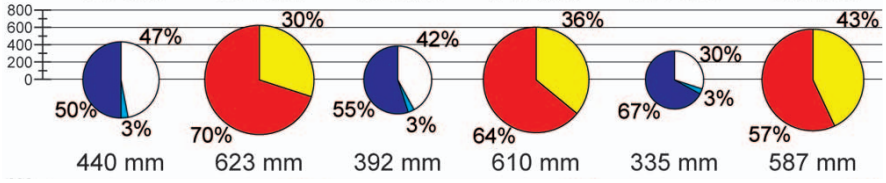						
Pangdo	16 496	2.0	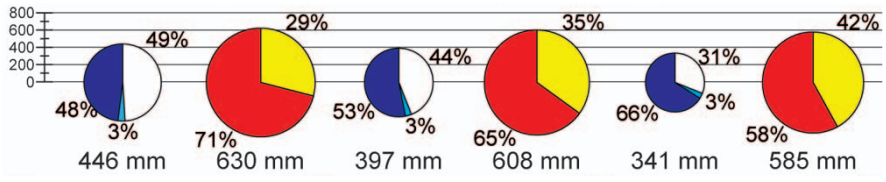						
Yang-bajing	2 719	11.5	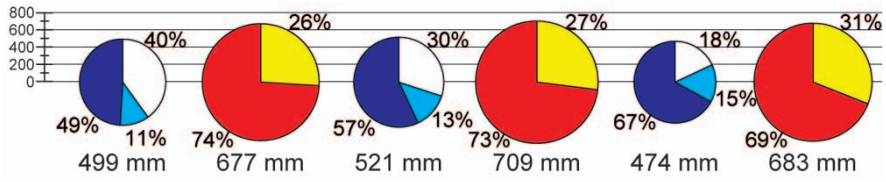						

radiation and snowmelt from its peak in early June. The decreasing rainfall and cloud cover towards the end of the rainy season in September and October cause snowmelt to increase again. Since glaciers are still protected by a snow cover, ice melt is not increasing. Falling temperatures in September decrease ice melt until it stops in late October. Accordingly, runoff generated from rainfall and ice melt is almost cyclic (see Sect. 2) at the outlet of the LRB. The close match between total modeled runoff with and without ice melt confirms the minor contribution of ice melt (Figs. 13, 16, S2). From the point of view of water management this is unfavorable since ice melt cannot augment low-flow conditions during the dry winter season.

The average seasonal course of runoff remains similar under assumed future climatic conditions (2011–2040, 2051–2080; Figs. 16b, c, S2). The main difference compared to the past is a clear decrease of the melt-water contribution from snow during summer and an increase in evapotranspiration. Increasing temperatures at all altitudes sharply reduce the amount of snowfall (Figs. 14, 15). The protective snow cover on glaciers is removed much earlier in the year by increasing snowmelt. Ice melt becomes the dominating melt contribution to runoff in early June, reaching a peak of 10 % at the basin outlet. The onset of the monsoon reduces ice melt from the glaciers as described above. Together with the glacier retreat the ice-melt contribution during summer

becomes lower in the scenario periods. Consequently, runoff is reduced, mainly caused by changes in the amount of precipitation. Additionally the reduction of snowmelt and increasing evapotranspiration forces the runoff reduction during early summer, particularly for the period from 2051 to 2080 (Figs. 16, S2).

These processes are basically similar for the sub-basin of Yangbajing with larger glacierization and accordingly larger ice-melt contribution to runoff (Figs. 16, right; S2, right). Although the amount of ice melt increases in future periods not only in spring as described above (Sects. 5.1, 5.2), but also in early summer, runoff is reduced during these months taking into account the increase in precipitation in the second scenario period. Only in May the increasing ice melt up to 30 % can augment the missing snowmelt and reduced precipitation, whereas during the summer months, this effect is negligible. Again, the strong decrease of snowmelt and increase of evapotranspiration are the reasons, despite higher altitudes and larger ice reservoirs with the described compensational effect (Sect. 5.1).

6 Conclusions

The presented approach offers the possibility to analyze the temporal and spatial pattern of the rainfall, snow- and ice-melt contribution to river runoff under past and future climatic conditions. The consideration of regional variations provides a detailed basis for the development of appropriate adaptation strategies to GCC in order to support future water availability. Although the models require a broad range of input data due to the complexity of the subject to be modeled, this study demonstrates their applicability in remote regions. The validation for the Lhasa River catchment presented proves the reliability of the model results for glaciers and for the hydrological water balance.

The resulting quantification of the contribution of glacier ice-melt water to river runoff not only in the highly glacierized head watersheds but also for the downstream regions as the main objective of this study let us conclude that ice melt, on average, has played and will play a minor role in the downstream water supply from the Lhasa River, contributing less than 5 %. Although glaciers will be strongly reduced by GCC, this is mainly due to the cyclic behavior of runoff generated from rainfall and from ice melt in the past and future in accordance to Thayyen and Gergan (2010), because precipitation and ice melt will remain cyclic under GCC according to the scenarios. Thus, the contribution of ice melt to total runoff will almost remain stable until 2080, although there will be a slight increase during a short period in spring. Contrary, the contribution of snowmelt to river runoff will generally decrease with GCC in the LRB and result in changes in water availability. Additionally, the increase of evapotranspiration with increasing air temperatures also will reduce water availability. Since the LRB is representative for glacierized, summer-monsoon dominated Himalayan basins, this result can be generalized for summer-monsoon dominated regions in the Himalayas as for instance the Ganges and Brahmaputra river basins (Fig. 1).

Uncertainties still exist in the simulation of future monsoon precipitation in current GCMs (Kripalani et al., 2007) and spatial distribution is still especially difficult to simulate (Kripalani et al., 2007; Dobler and Ahrens, 2010). Hence, significantly increased monsoon precipitation would modify the simulation result for runoff and glacier changes. Since there is no indication from the currently available climate model results that monsoon timing and dynamics will drastically change in the upcoming future as a consequence of GCC, the results of the study strongly suggest a re-evaluation of the future role of the glaciers for the water management in the Himalaya region and its lowlands.

Supplementary material related to this article is available online at: http://www.the-cryosphere.net/7/889/2013/tc-7-889-2013-supplement.pdf.

Acknowledgements. Financial support by the European Commission Sixth Framework Programme (FP6) within the project "Brahmatwinn" and the Federal Ministry of Education and Research (BMBF) within the "GLOWA-Danube" project are gratefully acknowledged. We thank the Institute of Tibetan Plateau Research ITP and the International Centre for Integrated Mountain Development ICIMOD for data provision.

Edited by: J. O. Hagen

References

Baraer, M., Mark, B. G., McKenzie, J. M., Condom, T., Bury, J., Huh, K., Portocarrero, C., Gómez, J., and Rathay, S.: Glacier recession and water resources in Peru's Cordillera Blanca, J. Glaciol., 58, 134–150, doi:10.3189/2012JOG11J186, 2012.

Barnett, T. P., Adam, J. C., and Lettenmaier, D. P.: Potential impacts of a warming on water availability in snow-dominated regions, Nature, 438, 303–309, doi:10.1038/nature04141, 2005.

Bolch, T., Yao, T., Kang, S., Buchroithner, M. F., Scherer, D., Maussion, F., Huintjes, E., and Schneider, C.: A glacier inventory for the western Nyainqentanglha range and the Nam Co basin, Tibet, and glacier changes 1976–2009, The Cryosphere, 4, 419–433, doi:10.5194/tc-4-419-2010, 2010.

Bolch, T., Kulkarni, A., Kääb, A., Huggel. C, Paul, F., Cogley, J. G., Frey, H., Kargel, J.S., Fujita, K., Scheel, M, Bajracharya, S., and Stoffel, M.: The State and Fate of Himalayan Glaciers, Science, 336, 310–314, 10.1126/science.1215828, 2012.

Bookhagen, B. and Burbank, D. W.: Toward a complete Himalayan hydrological budget: Spatiotemporal distribution of snowmelt and rainfall and their impact on river discharge, J. Geophys. Res., 115, F03019, doi:10.1029/2009JF001426, 2010.

Boston University: NASA TERRA/MODIS HDF-EOS MOD12Q1 V004 Land Cover Product Binary Data, Eurasia subset, IGBP Class Scheme, available at: http://duckwater.bu.edu/lc/mod12q1.html, 2004.

Casassa, G., López, P., Pouyaud, B., and Escobar, F.: Detection of changes in glacial run-off in alpine basins: examples from North America, the Alps, central Asia and the Andes, Hydrol. Process., 23, 31–41, doi:10.1002/hyp.7194, 2009.

Climate Limited-area Modeling Community, available at: http://www.clm-community.eu (last access: 22 May 2012), 2012.

Collins, D. N. and Taylor, D. P.: Variability of runoff from partially-glacierised Alpine basins, in: Hydrology in Mountains Regions, Proceedings of two Lausanne Symposia, August 1990, IAHS Publ., 193, 365–372, 1990.

Cruz, R. V., Harasawa, H., Lal, M., Wu, S., Anokhin, Y., Punsalmaa, B., Honda, Y., Jafari, M., Li, C., and Huu Ninh, N.: Asia, in: Climate Change 2007: Impacts, Adaptation and Vulnerability. Contribution of Working Group II to the Fourth Assessment Report of the Intergovernmental Panel on Climate Change, edited by: Parry, M. L., Canziani, O. F., Palutikof, J. P., van der Linden, P. J., and Hanson, C. E., Cambridge University Press, Cambridge, UK, 469–506, 2007.

Dobler, A. and Ahrens, B.: Precipitation by a regional climate model and bias correction in Europe and South Asia, Meteorolo. Z., 17, 499–509, doi:10.1127/0941-2948/2008/0306, 2008.

Dobler, A. and Ahrens, B.: Analysis of the Indian summer monsoon system in the regional climate model COSMO-CLM. Geophys. Res., 115, D16101, doi:10.1029/2009JD013497, 2010.

ERSDAC: The Ministry of Economy, Trade, and Industry (METI) of Japan and the United States National Aeronautics and Space Administration (NASA): Aster Global Digital Elevation Model (GDEM), available at: http://www.jspacesystems.or.jp/ersdac/GDEM/E/2.html, 2009.

FAO, IIASA, ISRIC, ISSCAS, JRC: Harmonized World Soil Database V 1.1, FAO, Rome, Italy and IIASA, Laxenburg, Austria, available at: http://www.iiasa.ac.at/Research/LUC/External-World-soil-database/HTML/, 2009.

Flügel, W.-A.: Twinning European and South Asian river basins to enhance capacity and implement adaptive integrated water resources management approaches – results from the EC-project BRAHMATWINN, Adv. Sci. Res., 7, 1–9, doi:10.5194/asr-7-1-2011, 2011.

Frauenfelder, R. and Kääb, A.: Glacier mapping from multitemporal optical remote sensing data within the Brahmaputra river basin, in: Proceedings of the 33rd International Symposium on Remote Sensing of Environment, Stresa, Italy, 4–8 May 2009, available at: http://folk.uio.no/kaeaeb/publications/299_R.Frauenfelder.pdf, 2009.

Garbrecht, J. and Martz, L. W.: TOPAZ Version 3.1, USDA, Agricultural Research Service Grazinglands Research Laboratory, Oklahoma, USA, 1999.

Haeberli, W. and Hoelzle, M.: Application of inventory data for estimating characteristics of and regional climate-change effects on mountain glaciers: a pilot study with the European Alps, Ann. Glaciol., 21, 206–212, 1995.

Huss, M.: Present and future contribution of glacier storage change to runoff from macroscale drainage basins in Europe, Water Resour. Res., 47, W07511, doi:10.1029/2010WR010299, 2011.

Huss, M., Farinotti, D., Bauder, A., and Funk, M.: Modelling runoff from highly glacierized alpine drainage basins in a changing climate, Hydrol. Process., 22, 3888-3902, doi:10.1002/hyp.7055, 2008.

Immerzeel, W. W., van Beek, L. P. H., and Bierkens, M. F. P.: Climate change will affect the Asian water towers, Science, 328, 1382–1385, doi:10.1126/science.1183188, 2010.

Immerzeel, W. W., van Beek, L. P. H., Konz, M., Shresta, A. B., and Bierkens, M. F. P.: Hydrological response to climate change in a glacierized catchment in the Himalayas, Climatic Change, 110, 721–736, doi:10.1007/s10584-011-0143-4, 2012.

Iziomon, M. G., Mayer, H., and Matzarakis, A.: Downward atmospheric longwave irradiance under clear and cloudy skies: Measurement and parameterization. J. Atmos. Sol-Terr. Phy., 65, 1107–1116, 2003.

Jansson, P., Hock, R., and Schneider, T.: The concept of glacier storage: a review, J. Hydrol., 282, 116–129, doi:10.1016/S0022-1694(03)00258-0, 2003.

Jarvis, A., Reuter, H. I., Nelson, A., and Guevara, E.: Hole-filled seamless SRTM data V3, International Centre for Tropical Agriculture (CIAT), available at: http://srtm.csi.cgiar.org, 2006.

Kääb, A., R. Frauenfelder, R., and Frauenfelder Kääb, J. A.: Glacier distribution and glacier area changes 1960s-2000 in the Brahmaputra river basin, EGU General Assembly, Vienna, Austria, 13–18 April 2008, EGU08–A–05334, 2008.

Kääb, A., Berthier, E., Nuth, Ch., Gardelle, J., and Arnaud, Y.: Contrasting patterns of early twenty-first-century glacier mass change in the Himalaya, Nature, 488, 495–498, doi:10.1038/nature11324, 2012.

Kaltenborn, B. P., Nellemann, C., and Vistnes, I. I.: High mountain glaciers and climate change. Challenges to human livelihoods and adaptation, United Nations Environment Programme, GRID-Arendal, Arendal, Norway, 56 pp., 2010.

Kang, S., Qin, D., Ren, J., Zhang, Y., Kaspari, S., Mayewski, P. A., and Hou, S.: Annual Accumulation in the Mt. Nyainqentanglha Ice core, Southern Tibetan Plateau, China: Relationships to Atmospheric Circulation over Asia, Arct. Antarct. Alp. Res., 39, 63–670, 2007.

Kaser, G., Großhauser, M., and Marzeion, B.: Contribution potential of glacierst o water availability in different climate regimes, P. Natl. Acad. Sci. USA, 107, 20223–20227, doi:10.1073/pnas.1008162107, 2010.

Kripalani, R. H., Oh, J. H., Kulkarni, A., Sabade, S. S., and Chaudhari, H. S.: South Asian summer monsoon precipitation variability: coupled climate simulations and projections under IPCC AR4, Theor. Appl. Climatol. 90, 133–159, doi:10.1007/s00704-006-0282-0, 2007.

Li, Z., He, Y., An, W., Song, L., Zhang, W., Catto, N., Wang, Y., Wang, S., Liu, H., Cao, W., Theakstone, W. H., Wang, S., and Du, J.: Climate and glacier change in southwestern China during the past several decades, Environ. Res. Lett., 6, doi:10.1088/1748-9326/6/4/045404, 2011.

Liston, G. E. and Elder, K.: A Meteorological Distribution System for High-Resolution Terrestrial Modeling (MicroMet), J. Hydrometeorol.,7, 217–234, 2006.

Marke, T.: Development and Application of a Model Interface to couple Regional Climate Models with Land Surface Models for Climate Change Risk Assessment in the Upper Danube Watershed, Ph.D. thesis, Ludwig-Maximilians-Universität Mu-

nich, Germany, available at: http://edoc.ub.uni-muenchen.de/9162/,188 pp., 2008.

Marke, T., Mauser, W., Pfeiffer, A., and Zängl, G.: A pragmatic approach for the downscaling and bias correction of regional climate simulations: evaluation in hydrological modeling, Geosci. Model Dev., 4, 759–770, doi:10.5194/gmd-4-759-2011, 2011a.

Marke, T., Mauser, W., Pfeiffer, A., Zängl, G., and Jacob, D.: The effect of downscaling on river runoff modeling: a hydrological case study in the Upper Danube Watershed, Hydrol. Earth Syst. Sc. Discuss., 8, 6331–6384, doi:10.5194/hessd-8-6331-2011, 2011b.

Mauser, W. and Bach, H.: PROMET – Large scale distributed hydrological modeling to study the impact of climate change on the water flows of mountain watersheds, J. Hydrol., 376, 362–377, doi:10.1016/j.jhydrol.2009.07.046, 2009.

Moore, R. D., Fleming, S. W., Menounos, B., Wheate, R., Fountain. A, Stahl, K., Holm, K., and Jakob, M.: Glacier change in western North America: Influences on hydrology, geomorphic hazards and water quality, Hydrol. Process., 23, 42–61, doi:10.1002/hyp.7162, 2009.

Nakićenović, N. and Swart, R.: IPCC Special Report on Emission Scenarios, Intergovernmental Panel on Climate Change, Cambrigde, United Kingdom, 608 pp., 2000.

Pellicciotti, F., Bauder, A., and Parola, M.: Effect of glaciers on streamflow trends in the Swiss Alps, Water Resour. Res., 46, W10522, doi:10.1029/2009WR009039, 2010.

Pellicciotti, F., Buergi, C., Immerzeel, W. W., Konz, M., and Shrestha, A. B.: Challenges and Uncertainties in Hydrological Modeling of Remote Hindu Kush-Karakoram-Himalayan (HKH) Basins: Suggestions for Calibration Strategie, Mt. Res. Dev., 32, 39–50, doi:10.1659/MRD-JOURNAL-D-11-00092.1, 2012.

Prasch, M., Bernhardt, M., Weber, M., Strasser, U., and Mauser, W.: Physically based modelling of snow cover dynamics in Alpine regions, in: Managing Alpine Future – IGF Forschungsberichte, 2, edited by: Borsdorf, A., Stötter, J., and Veulliet, E., Verlag der Österreichischen Akademie der Wissenschaften, Innsbruck, Austria, 322–330, 2008.

Prasch, M., Marke, T., Strasser, U., and Mauser, W.: Large scale integrated hydrological modelling of the impact of climate change on the water balance with DANUBIA, Adv. Sci. Res., 7, 61–70, doi:10.5194/asr-7-61-2011, 2011a.

Prasch, M., Weber, M., and Mauser, W.: Distributed modelling of snow- and ice-melt in the Lhasa River basin from 1971 to 2080, in: Cold Regions Hydrology in a Changing Climate, Proceedings of an international symposium, H02, held during IUGG 2011 in Melbourne, Australia, July 2011, IAHS Publ., 346, 57–64, 2011b.

Rees, H. G. and Collins, D. N.: Regional differences in response of flow in glacier-fed Himalayan rivers to climatic warming, Hydrol. Process., 20, 2157–2169, doi:10.1002/hyp.6209, 2006.

Sharma, K. P., Vorosmarty, Ch. J., and Moore III, B.: Sensitivity of the Himalayan hydrology to land-use and climatic changes, Climatic Change, 47, 117–139, 2000.

Singh, P., Arora, M., and Goel, N. K.: Effect of climate change on runoff of a glacierized Himalayan basin, Hydrol. Process., 20, 1979–1992, doi:10.1002/hyp.5991, 2006.

Thayyen, R. J. and Gergan, J. T.: Role of glaciers in watershed hydrology: a preliminary study of a "Himalayan catchment", The Cryosphere, 4, 115–128, doi:10.5194/tc-4-115-2010, 2010.

Viviroli, D., Dürr, H. H., Messerli, B., Meybeck, M., and Weingartner, R.: Mountains of the world, water towers for humanity: Typology, mapping, and global significance, Water Resour. Res., 43, W07447, doi:10.1029/2006WR005653, 2007.

Viviroli, D., Archer, D. R., Buytaert, W., Fowler, H. J., Greenwood, G. B., Hamlet, A. F., Huang, Y., Koboltschnig, G., Litaor, M. I., López-Moreno, J. I., Lorentz, S., Schädler, B., Schreier, H., Schwaiger, K., Vuille, M., and Woods, R.: Climate change and mountain water resources: overview and recommendations for research, management and policy, Hydrol. Earth Syst. Sc., 15, 471–504, doi:10.5194/hess-15-471-2011, 2011.

Weber, M., Braun, L. N., Mauser, W., and Prasch, M.: Contribution of rain, snow- and icemelt in the upper Danube today and in the future, Geogr. Fis. Din. Quat., 33, 221–230, 2010.

World Data Center For Glaciology and Geocryology: Chinese Glacier Inventory, available at: http://wdcdgg.westgis.ac.cn/ (last access: 17 August 2009), 2009.

Xu, J., Grumbinde, R. E., Shrestha, A., Eriksson, M., Yang, X., Wang, Y., and Wilkes, A.: The Melting Himalayas: Cascading Effects of Climate Change on Water, Biodiversity, and Livelihoods, Conserv. Biol., 23, 520–530, doi:10.1111/j.1523-1739.2009.01237.x, 2009.

Yao, T., Pu, J., and Liu, S.: Changing glaciers in High Asia, in: Glacier science and environmental change, edited by: Knight, P.G., Wiley, Oxford, United Kingdom, 275–282, 2006.

Yao, T., Pu, J., Lu, A., Wang, Y., and Yu, W.: Recent glacial retreat and its impact on hydrological processes on the Tibetan Plateau, China, and surrounding regions, Arct. Antarct. Alp. Res., 39, 642–650, doi:10.1657/1523-0430(07-510)[YAO]2.0.CO;2, 2007.

Zhou, C., Wenbin, Y., Wu, L., and Liu, S.: Glacier changes from a new inventory, Nianchu river basin, Tibetan Plateau, Ann. Glaciol., 50, 87–92, doi:10.3189/172756410790595868, 2010.